Mössbauer studies of magnetic phase transitions in the alloy series $(Fe_{1-x}Mn_x)_3Ga_1$

1998 J. Phys.: Condens. Matter 10 6135

(http://iopscience.iop.org/0953-8984/10/27/014)

J. Phys.: Condens. Matter **10** (1998) 6135–6146. Printed in the UK PII: S0953-8984(98)91452-7

Mössbauer studies of magnetic phase transitions in the alloy series $(Fe_{1-x}Mn_x)_3Ga_4$

J A Hutchings†, M F Thomas†, H J Al-Kanani‡ and J G Booth‡

† Department of Physics, University of Liverpool, Liverpool L69 7ZE, UK
‡ Department of Physics, University of Salford, Salford M5 4WT, UK

Received 9 February 1998, in final form 23 April 1998

Abstract. The crystal structure of the parent alloy Fe_3Ga_4 of the series under investigation has four distinct iron sites. Mössbauer spectra of the series $(Fe_{1-x}Mn_x)_3Ga_4$ with $0 \leqslant x \leqslant 0.2$ recorded at 293 and 4.2 K and fitted with four components show little site preference for Mn substitution up to $x = 0.15$. At $x = 0.20$ evidence for site preference is observed. The magnetic phases at 4.2 K were deduced from changes in the Mössbauer spectra in applied fields. The alloy with $x = 0.20$ is found to be ferromagnetic. Alloys with $x = 0.05$, 0.10 and 0.15 show evidence of a canted spin phase. A transition from a canted to a ferromagnetic phase is observed at applied fields $B \approx 5$ T for the $x = 0.15$ alloy. Phase diagrams constructed from Mössbauer and magnetization results are compared with the predictions of a generalized theoretical model which incorporates ferromagnetic and antiferromagnetic interactions.

1. Introduction

The crystal structure of Fe_3Ga_4 has been determined by Philippe *et al* [1]. The unit cell contains eighteen iron atoms occupying four inequivalent sites in proportions A (2), B (4), C (4) and D (8). Magnetization measurements show complex behaviour [2]; below 20 K the alloy behaves as a ferromagnet but above this temperature the behaviour in weak fields reveals antiferromagnetism with a Néel temperature $T_N = 392$ K. This magnetic behaviour has been compared with the theory of Moriya and Usami [3] and Isoda [4] which makes general predictions for itinerant electron magnets in which ferromagnetic and antiferromagnetic interactions coexist and the resultant phase—ferromagnetic, antiferromagnetic or coexistence (canted phase or ferrimagnetic) depends on the relative strengths of the interactions and the strength of the coupling between modes.

In an extension to the study of Fe_3Ga_4, the alloy series $(Fe_{1-x}Mn_x)_3Ga_4 : 0 \leqslant x \leqslant 0.2$ has been studied by magnetization measurements [5]. The results indicate a low temperature–low field antiferromagnetic state for $0.05 \leqslant x \leqslant 0.15$ but with increasing x the transition to a ferromagnetic state occurs at progressively lower temperature and the $x = 0.20$ alloy is observed to be ferromagnetic down to 2 K—the lowest temperature measured.

The present Mössbauer investigation was undertaken to complement the magnetization results by obtaining spectra giving evidence on site selectivity of the Mn for Fe substitution and the evolution of spin directions on Fe sites in increasing applied magnetic fields at 4.2 K. Results from the analyses of the spectra are aimed at identifying magnetic phases and detecting phase transitions.

0953-8984/98/276135+12$19.50

2. Experimental technique

The alloy samples were made by argon arc melting as detailed by Al-Kanani and Booth [5]. X-ray measurements showed the alloys to be single phase with the same crystal structure as Fe_3Ga_4 and comparable lattice dimensions. Mössbauer samples were made by mixing optimum quantities of the powdered alloy ($\sim$24 mg cm^{-2}) calculated for maximum signal to noise [6] with boron nitride powder which provides even distribution and random grain orientation. Mössbauer spectra were taken on conventional absorption spectrometers featuring a double ramp waveform where the absorption spectra appear on a flat background after combining subspectra taken with velocity increasing and velocity decreasing ramps. Sources of ^{57}Co in Rh of strengths up to 100 mCi were used with the gamma radiation detected with longitudinal proportional counters filled with Ar/CH_4 having 67% efficiency for the 14.4 keV Mössbauer radiation. The spectrometers were calibrated with 25 μm iron foils and isomer shift values are quoted relative to α-iron at 293 K. Spectra with applied fields in the range $0 \leqslant B \leqslant 13$ T were taken using a superconducting magnet of solenoidal geometry with the gamma-ray beam parallel to the applied field. Field broadening of the absorption lines is minimized by a reverse wound coil at the source position that cancels the main field at this point. Experiments determining the magnetic ordering temperatures used a Mössbauer spectrometer incorporating a furnace controlled by a thermocouple. The alloy/BN samples for these spectra were enclosed in Al sample holders giving a temperature uniformity and stability of 0.5 K over the one day counting period.

3. Results and analysis

Mössbauer spectra were taken for alloys with $x = 0$, 0.05, 0.10, 0.15 and 0.20 in zero applied field at 293 K and 4.2 K. At 4.2 K spectra were taken for the alloys in applied fields up to 13 T and for the alloys $x = 0$, 0.10 and 0.20 spectra were taken in zero applied field in the temperature range 293–430 K. The high temperature series of spectra established magnetic ordering temperatures for the alloys as the hyperfine fields collapsed. For alloys $x = 0$, 0.10 and 0.20 ordering temperatures of 395 ± 5 K, 417 ± 2 K and 412 ± 2 K respectively were obtained. The value for the parent alloy Fe_3Ga_4 ($x = 0$) is in excellent agreement with that (392 K) determined by Kawamiya and Adachi [2]. The zero field spectra at 293 K showed no features not observed more clearly at 4.2 K; the analysis was thus concentrated on the 4.2 K spectra.

The spectra at 4.2 K are shown in figure 1 fitted to four components corresponding to the four distinct crystal sites. In pure Fe_3Ga_4 the site occupation is A (11%), B (22%), C (22%) and D (45%) where the site convention is consistent with that of Kawamiya and Adachi [2]. In fitting the spectra random orientation of the alloy gains is assumed requiring that the relative intensities of the outer, middle and inner doublet components of the magnetic sextet pattern have area ratios 3:2:1. Values of isomer shift, quadrupole shift, hyperfine field and relative area for each component are allowed to vary. In the fits the values of isomer shift for all components of all the samples lie in the narrow range 0.40–0.45 mm s^{-1} (relative to α-iron at 293 K) with no systematic trend with x. Values of quadrupole shift are all near zero, lying in the range 0.0 ± 0.10 mm s^{-1}. The main parameter that distinguishes iron atoms on different sites is the hyperfine field, B_{hf}, and fitted values of this parameter are listed for each component in table 1, together with the linewidth Γ and the percentage area of the components. The fits to the spectra in figure 1 show that for $x \leqslant 0.20$ satisfactory fits are obtained with four components. The values listed in table 1 show that Mn substitution does not increase the linewidth appreciably. The relative areas of components change but

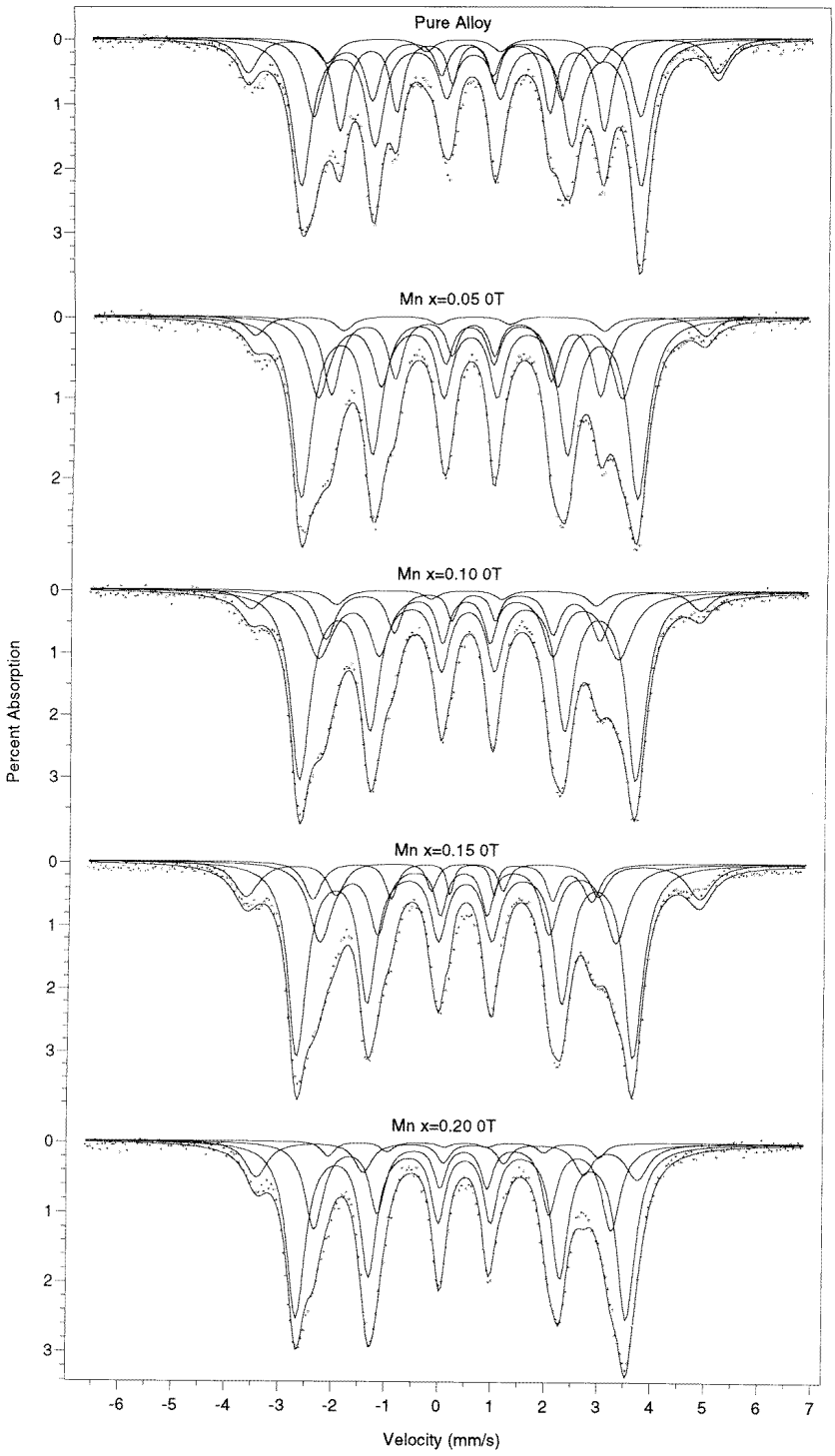

Figure 1. Spectra of alloys $(Fe_{1-x}Mn_x)_3Ga_4$ at 4.2 K with $x = 0.0$, 0.05, 0.10, 0.15 and 0.20. The spectra are fitted with four components whose areas match the population of iron atoms on the four distinct crystal sites.

Table 1. Values of hyperfine field B_{hf} in kG, linewidth Γ in mm s^{-1} and area I in per cent for the four fitted components of the alloys with $x = 0.05$, 0.10, 0.15 and 0.20 shown in figure 1. Typical errors in hyperfine field values are ±4 kG, in linewidths ±0.04 mm s^{-1} and in areas ±4%.

	$x = 0.05$			$x = 0.10$			$x = 0.15$			$x = 0.20$		
Site	B_{hf}	Γ	I	B_{hf}	Γ	I	B_{hf}	Γ	I	B_{hf}	Γ	I
A	262	0.34	11	261	0.33	11	261	0.35	6	224	0.32	14
B	181	0.37	22	182	0.38	22	180	0.38	30	173	0.40	27
C	159	0.36	22	162	0.41	22	160	0.42	16	159	0.30	4
D	198	0.39	45	198	0.39	45	197	0.39	48	193	0.39	55

the spectra do not require fitting with more than four components. In fact the spectra do not show large variation with increasing x, the main change being that the absorption line at $\sim +3$ mm s^{-1} in the spectrum of Fe_3Ga_4 becomes progressively less intense as x increases. This line arises from the component of site C. In the range $0.05 \leqslant x \leqslant 0.15$ the relative area of the site C component remains essentially constant as increased width of the peak compensates for the reduction in intensity. However in the fit to the $x = 0.20$ alloy the reduction in the area of the site C component and the increase in that of site D indicates preferred substitution of Mn onto site C at the expense of site D.

Mössbauer spectra at 4.2 K showing the response of the powder samples with $x = 0.05$, 0.10, 0.15 and 0.20 to an applied field B directed parallel to the gamma-ray beam are displayed in figures 2, 3, 4 and 5 respectively. In fitting these spectra the relative component areas for a given value of x are determined by the zero field spectrum and are kept constant at all other fields. In an applied field B the effective field B_{eff} observed in the Mössbauer spectrum is related to the hyperfine field B_{hf} by the relation:

$$B_{eff} = \{B^2 + B_{hf}^2 - 2BB_{hf}\cos\theta\}^{1/2}$$

where θ is the angle between the magnetic moments of the iron atoms and the applied field. The Mössbauer spectrum gives information on B_{eff} for each component and independently on the angle θ via the value R in the relative intensities of the outer, middle and inner doublets of the magnetic sextet component which can be represented as $3{:}R{:}1$ where $R = 4\sin^2\theta/(1 + \cos^2\theta)$. Values of B_{eff} and R are varied but are constrained by the relation above. The linewidths of the fitted components show little increase as the applied field is increased. Typically, in the $x = 0.10$ alloy increase of field from zero to 10 T results in linewidth increases of 13%, 8%, 17% and 20% for A, B, C, and D sites respectively. This indicates that the intrinsic magnetic anisotropy energies are smaller than applied field energies and that the spin directions are effectively defined by the angle θ irrespective of grain orientation.

The most straightforward sequence of spectra to interpret is for $x = 0.20$, shown in figure 5. In zero field the randomly directed moments give rise to sextet components with $R = 2$. The increase of applied field causes a rapid decrease in R corresponding to alignment of magnetic moments parallel to the field. Complete alignment, corresponding to $\theta = 0$, is seen to be achieved at $B > 2$ T. Further increase in field to $B = 8$ T and $B = 13$ T results in decrease in effective field B_{eff} since the hyperfine field B_{hf} (kept constant at the zero field value) is directed opposite to the atomic magnetic moment and is thus directly opposed to the applied field giving $B_{eff} = B_{hf} - B$. The behaviour for $B > 2$ T must correspond to ferromagnetic order as the only other structure showing collinear moment

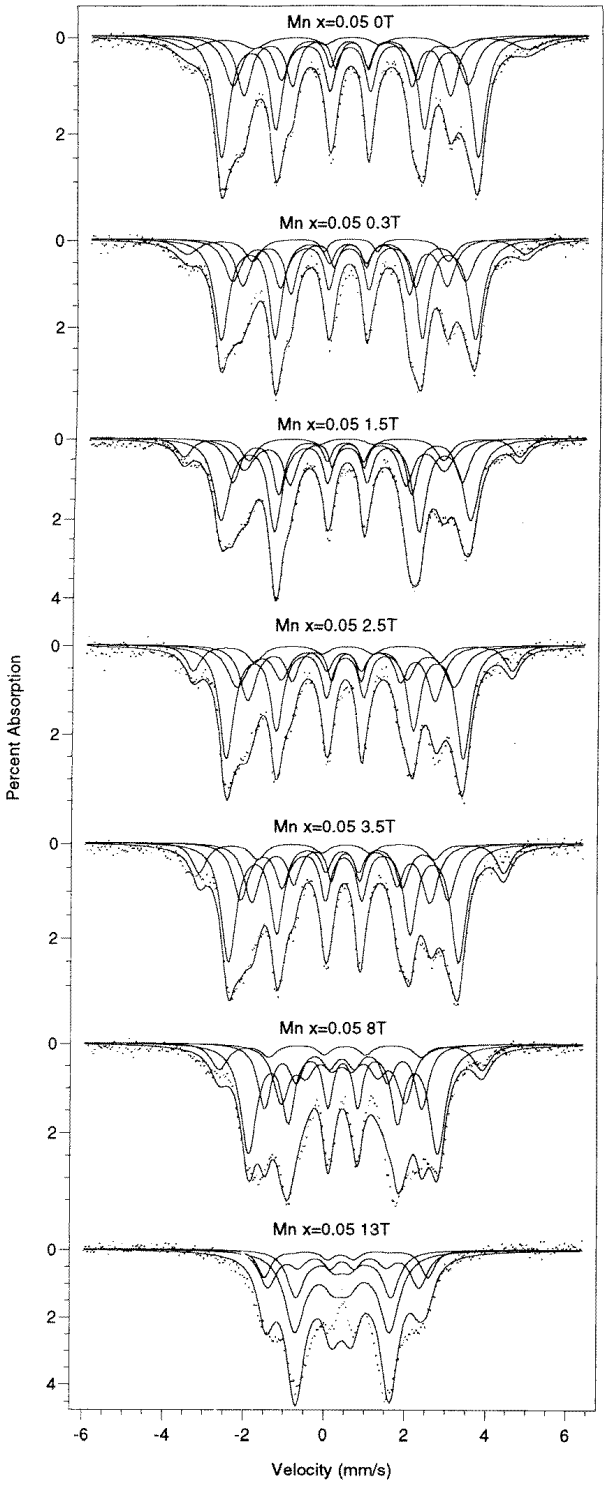

Figure 2. Spectra of the alloy $(Fe_{0.95}Mn_{0.05})_3Ga_4$ at 4.2 K in applied fields if up to 13 T directed parallel to the gamma-ray beam. The spectra are fitted in a similar way to those above.

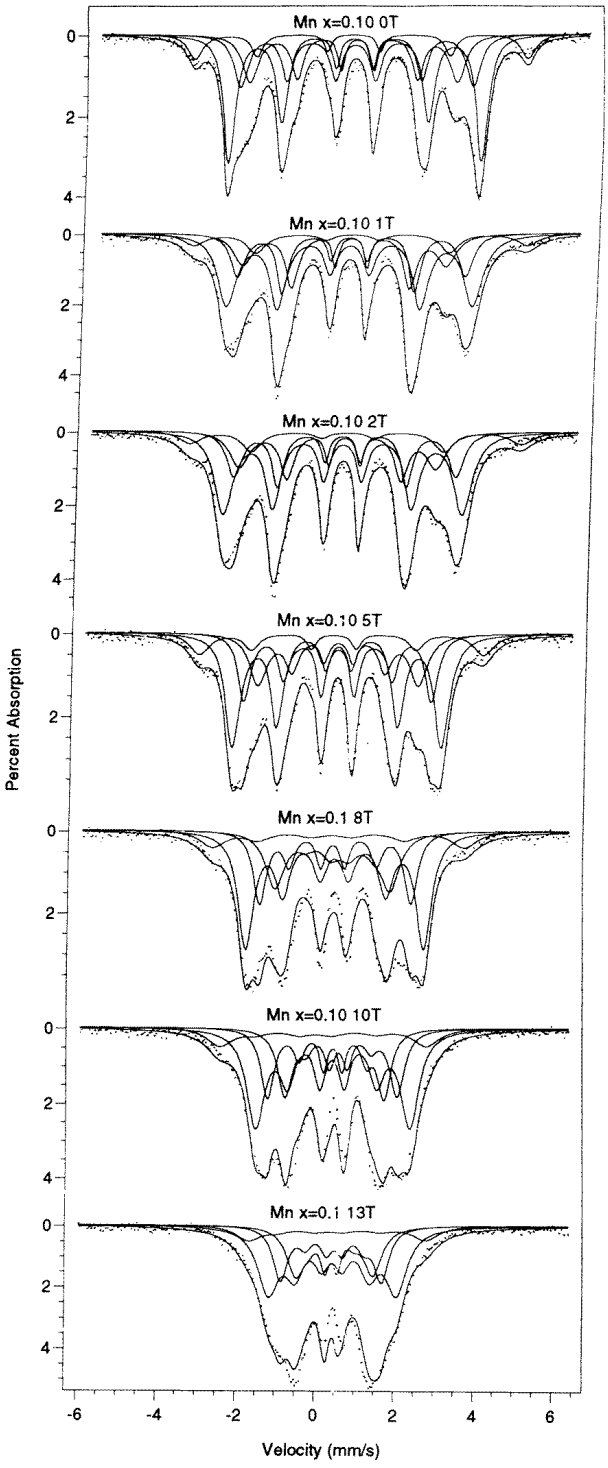

Figure 3. Spectra of the alloy $(Fe_{0.90}Mn_{0.10})_3Ga_4$ at 4.2 K in fields of up to 13 T directed parallel to the gamma-ray beam. The spectra are fitted in a similar way to those above.

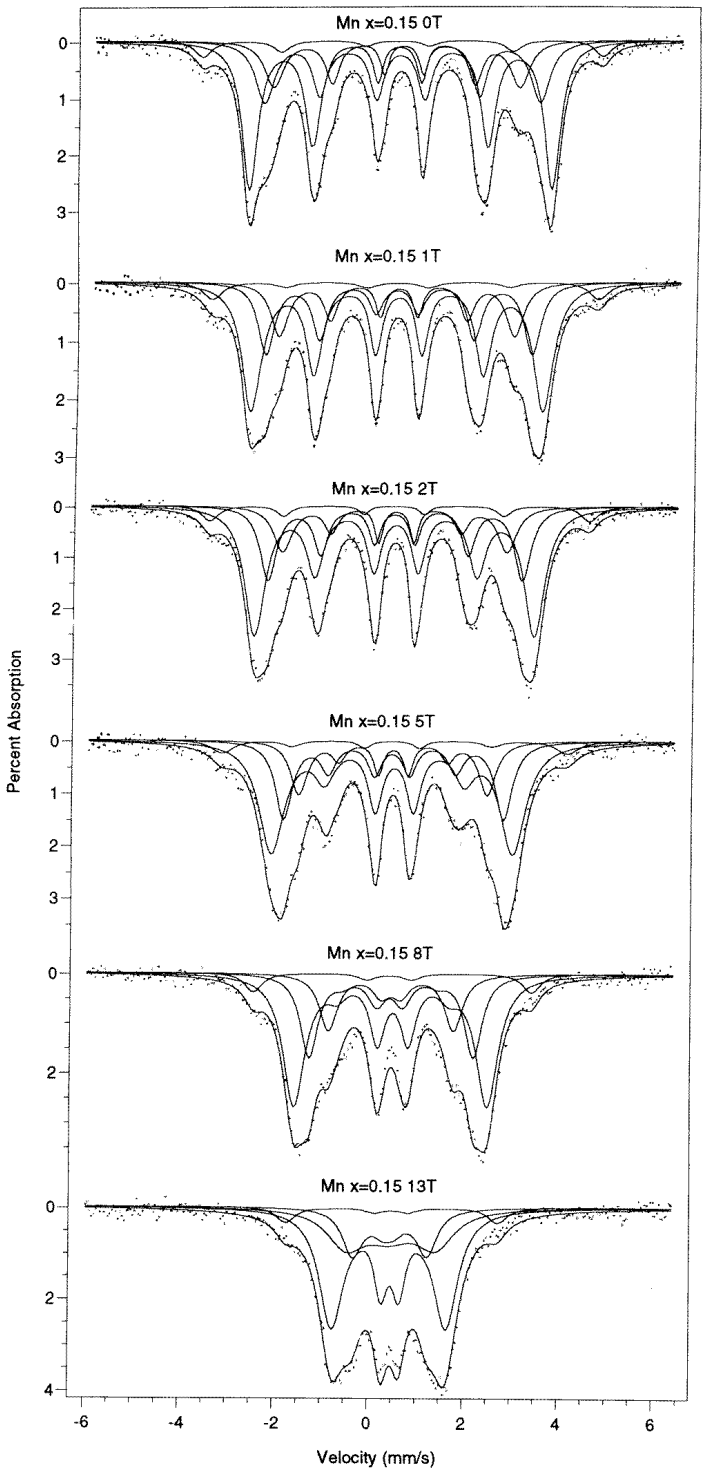

Figure 4. Spectra of the alloy $(Fe_{0.85}Mn_{0.15})_3Ga_4$ taken at 4.2 K in the same geometry as above. The spectra are fitted in a similar manner.

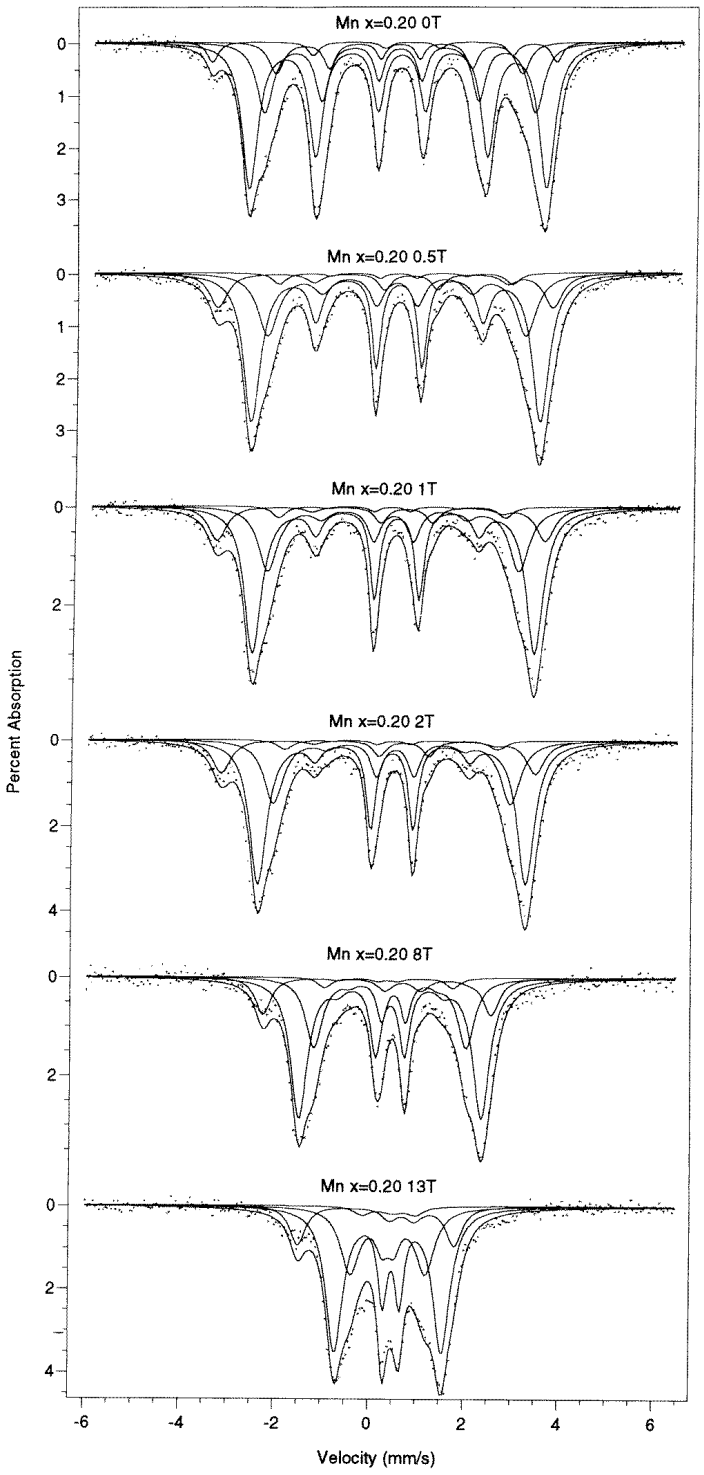

Figure 5. Spectra of the alloy $(Fe_{0.80}Mn_{0.20})_3Ga_4$ taken and fitted in the same manner as those in the previous figures.

alignment, ferrimagnetic, would also include a component whose effective field B_{eff} would increase with applied field. In the spectra for $B = 0.5$, 1.0 and 2.0 T the presence of some intensity in the middle doublet of the magnetic sextet indicates that the spins are not completely parallel with the applied field as expected for a ferromagnetic state. A possible explanation is that in this range of field the spins are in a (highly) canted structure that does not change to a ferromagnetic state until $B > 2$ T.

For the sample with $x = 0.15$ the spectrum at $B = 13$ T is seen to be similar to that for the $x = 0.20$ ferromagnetic alloy at the same field. At high field the $x = 0.15$ alloy is ferromagnetic. At low fields, however, values of R do not decrease until $B = 2$ T and only decrease substantially at $B = 5$ T with accompanying decrease of effective field B_{eff}. Alignment of magnetic moments has not occurred at $B = 1$ T and is small at $B = 2$ T. The behaviour indicates a ferromagnetic state occurring at $B \geqslant 5$ T. At $B \leqslant 2$ T the spectra indicate antiferromagnetic structure, either as a pure antiferromagnetic state or a canted state with antiferromagnetism and ferromagnetism occurring along perpendicular axes. In figure 6 the angles θ between the directions of the spins and the applied field for the sites A, B, C and D are plotted against the applied field strength. The overall trend of θ against B supports the picture of alignment into a ferromagnetic phase in the range $5\text{ T} < B < 8\text{ T}$.

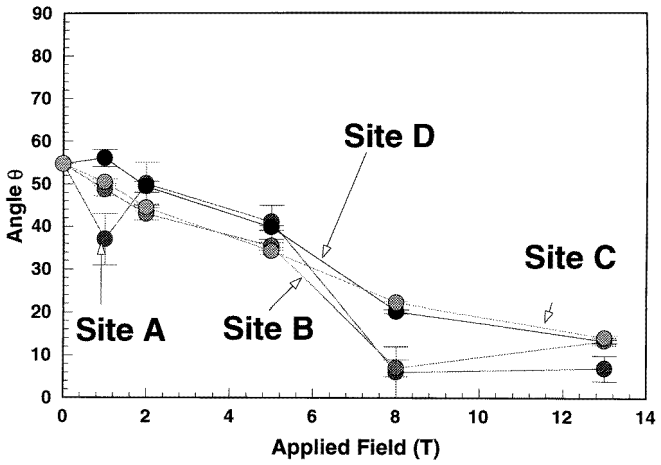

Figure 6. Graph of angles θ versus applied field for sites A, B, C, D in the $x = 0.15$ alloy. Angle θ is that between the spin direction and the applied field.

The change of Mössbauer spectra with increasing field for the alloys with $x = 0.05$ and $x = 0.10$ follows a similar pattern. As the applied field is increased up to $B = 1.5$ T values of R increase corresponding to an increase in the perpendicular components of magnetic moments with respect to the beam. At higher values of applied field the reduction in the values of R indicates increased alignment of moments in the gamma-ray direction and, for $B = 8$ T and above, the characteristic decrease in B_{eff} corresponds to a high degree of alignment of moments to the applied field. The increase in perpendicular spin components for $B \leqslant 2.5$ T could be due to spin flop alignment of a pure antiferromagnet but is more likely to be the result of alignment of a canted system where the field aligns the weak ferromagnetic moment leaving the mainly antiferromagnetic spin directions normal to the field. For applied fields $B \geqslant 8$ T reduction in B_{eff} is observed corresponding to alignment of moments with the field but the spectra are seen to be different from those of the ferromagnetic phase seen for the $x = 0.15$ and $x = 0.20$ alloys at high values of

applied field. We deduce that for the alloys $x = 0.05$ and 0.10 the canted phase persists up to $B = 13$ T. For the spectra of the canted phase, particularly for $B \geqslant 8$ T, it was impossible to obtain good fits if the hyperfine fields, B_{hf}, were kept constant at the values observed in the zero field spectrum. The fits dictated that the values of B_{hf} decreased as the values of the applied field B increased. The spectra of the $x = 0.05$ and $x = 0.10$ alloys for $B = 13$ T are not well fitted and indicate that the canted phase picture may not be applicable. A possible explanation is that this canted phase may be undergoing a transition to the field driven paramagnetic state. This would be consistent with the reduction in hyperfine field necessary in the existing fits. The exact nature of the magnetic structure of these alloys in such conditions, however, remains unsolved.

A difficulty in extracting information from fits to the spectra occurs because of the complexity caused by the four components each with a number of variable parameters. It is therefore valuable to have a check that the fits are consistent with other experimental results. Such a check is provided by constructing an M versus B magnetization curve from the fits by evaluating the relative magnetization M as

$$M = \sum_{n=1}^{4} A_n \cos\theta_n$$

where A_n is the relative area of component n and θ_n is obtained from the Mössbauer line intensity ratio R. This Mössbauer generated magnetization is shown in figure 7. The points assume equal magnetic moments at each site but essentially identical results are obtained by multiplying each term by a magnetic moment term—taken to be proportional to the hyperfine field at the site. The overall shape of the curves, which show good agreement with the measured curves of Al-Kanani and Booth [5], can be taken as confirmation of the Mössbauer fits.

4. Discussion

The series of spectra illustrated in figures 2 to 5 shows that canted spin and ferromagnetic phases can be distinguished. In the ferromagnetic phase the spectra at all values of applied field are well fitted keeping the hyperfine field B_{hf} constant at its zero applied field value. However for the canted spin system the fits require that the value of B_{hf} decreases with increasing applied field B. This was particularly noticeable for $B \geqslant 8$ T. The canting angles θ of the spins to the applied field (parallel to the gamma ray beam) are reflected in the values of R and are seen to decrease with increasing B. This increased alignment is not thought to be a consequence of direct interaction with the applied field as ordering temperatures $T_C \sim 400$ K correspond to exchange field values $\sim$700 T, too large for applied field values $B \leqslant 13$ T to cause appreciable canting. The increased canting observed in the spectra as the field is increased indicates an increase in the relative values of ferromagnetic to antiferromagnetic coupling strengths which decrease the effective antiferromagnetic exchange strength and culminate in a transition to the ferromagnetic state.

The results are summarized in the schematic phase diagrams shown in figure 8. In figure 8(a) the magnetic phases observed at 4.2 K for different values of applied field and Mn doping levels, x, are shown. In the figures A, C, F refer to antiferromagnetic, canted spin and ferromagnetic phases respectively. The Mössbauer results are used to establish the phase boundary between canted spin and ferromagnetic states. In addition the magnetization results of Al-Kanani and Booth [5] are used to define a region of antiferromagnetism at low applied field where the Mössbauer data are not sensitive. Magnetization results [2]

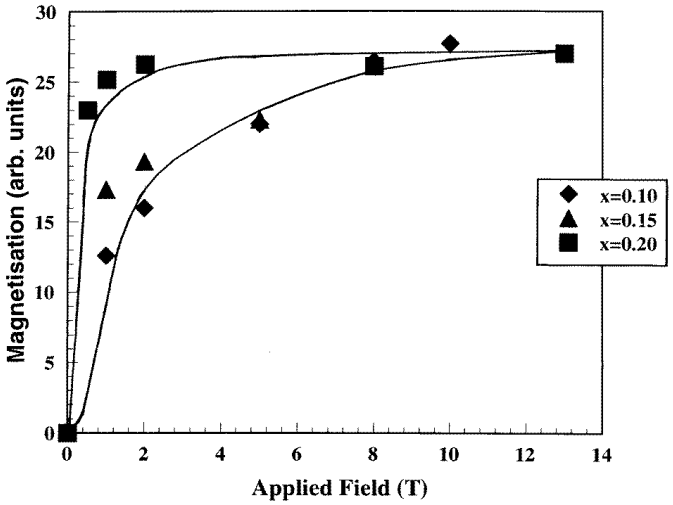

Figure 7. Graphs of relative magnetization M versus applied field B for alloys with $x = 0.10$, 0.15 and 0.20. The values of M are evaluated from fits to the Mössbauer spectra using the expression in the text. The lines are from the magnetization curves of [5] for $x = 0.10$ and $x = 0.20$ alloys, scaled to the value at 12 T.

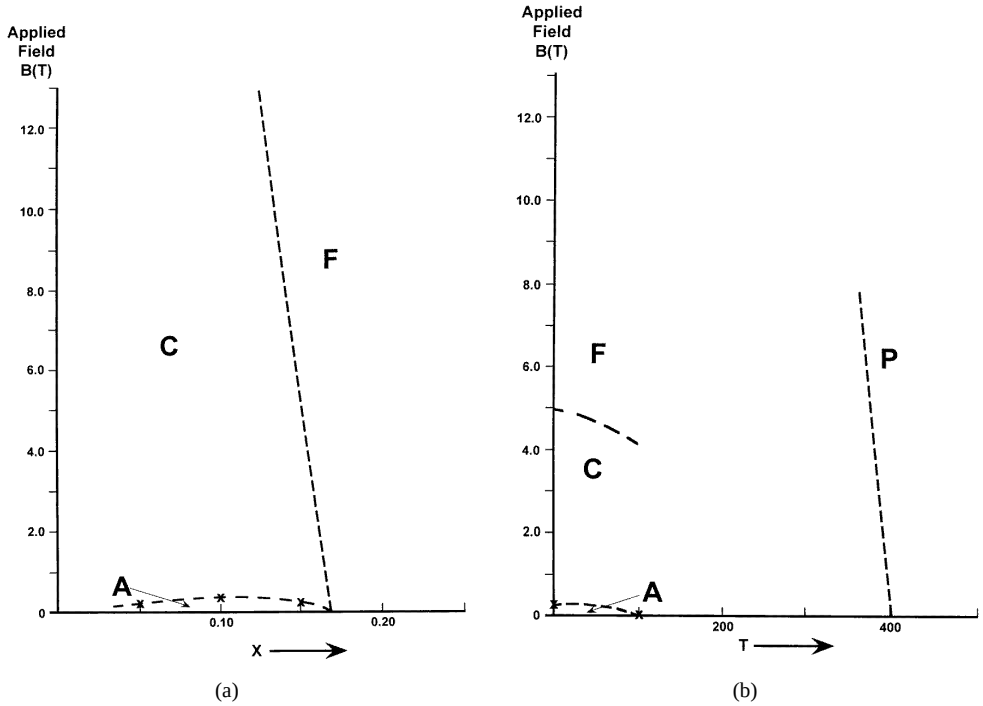

Figure 8. (a) Schematic applied field B–doping level x diagram of magnetic phases at 4.2 K constructed from the Mössbauer and magnetization results. Antiferromagnetic canted spin and ferromagnetic phases are denoted by A, C and F respectively. (b) Schematic applied field B–temperature T diagram of magnetic phases for the $x = 0.15$ alloy constructed from the Mössbauer and magnetization results. P denotes the paramagnetic phase.

indicate that at 4.2 K the parent compound Fe_3Ga_4 is ferromagnetic. This does not agree with the sequence of Mössbauer spectra taken in applied fields in this work. This sequence, essentially similar to those illustrated for $x = 0.05$ and $x = 0.10$ alloys, indicates a canted spin phase. In figure 8(b) the phase diagram of applied field B versus temperature T is shown for the $x = 0.15$ alloy. It is seen that at 4.2 K increasing field drives the magnetic phase through the sequence antiferromagnetism $\rightarrow$ canted spin $\rightarrow$ ferromagnetism.

A phase diagram similar to that constructed by these empirical results is predicted by Isoda [4] from a theoretical model incorporating coexistence of antiferromagnetic and ferromagnetic interactions. The sequence of phases observed requires conditions for this model that $T_C > T_N$ and the coefficient γ_S for the staggered antiferromagnetic magnetization M_Q^4 be greater than the coefficient γ_U of the ferromagnetic magnetization M_0^4.

Acknowledgments

We wish to acknowledge Michael Attenborough for his work in developing the program that fits the spectra taken in applied field and incorporates the relation between effective field and line intensities.

J A Hutchings acknowledges the support of an EPSRC research studentship.

References

[1] Philippe M J, Malaman B, Roques B, Courtois A and Protas J 1975 *Acta Crystallogr.* B **31** 477–82
[2] Kawamiya N and Adachi K 1986 *J. Phys. Soc. Japan* **55** 634–40
[3] Moriya T and Usami K 1977 *Solid State Commun.* **23** 935–8
[4] Isoda M 1984 *J. Phys. Soc. Japan* **53** 3587–98
[5] Al-Kanani H J and Booth J G 1995 *Physica* B **211** 90–2
[6] Long G, Longworth G and Cranshaw T E 1983 *Mössbauer Effect Data J.* **6** 42–9